High Frequency of PDGFRA and MUC Family Gene Mutations in Diffuse Hemispheric Glioma, H3 G34-mutant: A Glimmer of Hope?

Wanming Hu
Sun Yat-sen University Cancer Center https://orcid.org/0000-0002-3632-1258
Hao Duan
Sun Yat-sen University Cancer Center
Sheng Zhong
Sun Yat-sen University Cancer Center
Jing Zeng
Sun Yat-sen University Cancer Center
Yonggao Mou (mouyg@sysucc.org.cn)
Sun Yat-sen University Cancer Center

Research Article

Keywords: diffuse hemispheric glioma, H3G34R/V, H3K27M, PDGFRA, MUC, immune infiltration, Survival

Posted Date: November 12th, 2021

DOI: https://doi.org/10.21203/rs.3.rs-904972/v1

Version of Record: A version of this preprint was published at Journal of Translational Medicine on February 2nd, 2022. See the published version at https://doi.org/10.1186/s12967-022-03258-1.

Abstract

Background

Diffuse hemispheric glioma H3 G34-mutant (G34-DHG) is a new type of pediatric-type diffuse high-grade glioma in the fifth edition of the WHO Classification of Tumors of the Central Nervous System. The current treatment for G34-DHG involves a combination of surgery and conventional radiotherapy or chemotherapy; however, the therapeutic efficacy of this approach is not satisfactory. In recent years, molecular targeted therapy and immunotherapy have achieved significant benefits in a variety of tumors. In-depth understanding of molecular changes and immune infiltration in G34-DHGs will help to establish personalized tumor treatment strategies. Here, we report the clinicopathological, molecular and immune infiltration characteristics of G34-DHG cases from our center along with cases from the HERBY Trial and the Chinese Glioma Genome Atlas database (CGGA).

Methods

Hematoxylin-eosin (HE) and immunohistochemistry (IHC) staining were used to present the clinicopathological characteristics of 10 Chinese G34-DHG patients treated at our institution. To address the molecular characteristics of G34-DHG, we performed whole-exome sequencing (WES) and RNA sequencing (RNA-seq) analyses of 5 patients from our center and 3 Chinese patients from the Chinese Glioma Genome Atlas (CGGA) database. Additionally, 7 European G34-DHG patients from the HERBY Trail were also subjected to analyses, with 7 cases of WES data and 2 cases of RNA-seq data.

Results

WES showed a high frequency of *PDGFRA* mutation in G34-DHGs (12/15). We further identified frequent mutations in *MUC* family genes in G34-DHGs, including *MUC16* (8/15) and *MUC17* (8/15). Although no statistical difference was found, *PDGFRA* mutation tended to be an indicator for worse prognosis whereas *MUC16*/*MUC17* mutation indicated a favorable prognosis in G34-DHGs. RNA sequencing results revealed that most G34-DHG are considered to be immune cold tumors. However, one patient in our cohort with *MUC16* mutation showed significant immune infiltration, and the total overall survival of this patient reached 75 months.

Conclusions

Our results demonstrate that G34-DHG is a new high-grade glioma with high frequency of *PDGFRA* and *MUC* gene family mutations. PDGFRA may serve as an indicator of poor prognosis and an effective therapeutic target. Moreover, *MUC16* tends to be a favorable prognostic factor and indicates high immune infiltration in certain patients, and these findings may provide a new direction for targeted therapy and immunotherapy of patients with G34-DHGs.

Background

Pediatric-type diffuse high-grade glioma (pHGG) is a highly aggressive brain tumor with a poor prognosis that accounts for approximately 8%–15% of all central nervous system tumors in children and adolescents [1]. The widespread use of high-throughput sequencing, genetic profiling and epigenetic analysis has greatly increased our understanding of the cell origin, pathogenesis and biological characteristics of pHGG. Two types of heterozygous somatic mutations in *H3F3A*, which encodes histone H3, were firstly identified in pHGG in 2012 [2]. These mutations lead to an amino acid substitution at key residues (K27M or G34R/G34V). Subsequent studies found that K27M mutation presented in both H3F3A and HIST1H3B/C genes, but G34R/V-mutant gliomas were characterized by recurrent glycine-to-arginine/valine alterations at codon 34 (G34R/V) only in the H3F3A gene. The fifth edition of the WHO Classification of Tumors of Central Nervous System in 2021 defined the standard name of G34R/V-mutant gliomas as diffuse hemispheric glioma H3 G34-mutant, classified as WHO grade 4.

Most diffuse hemispheric glioma H3 G34-mutant tumors (G34-DHGs) carry *TP53* mutations and *ATRX* deletions [2], with hypermethylation at the OLIG2 locus, leading to the absence of OLIG2 expression [3]. The current treatment for these tumors is surgery, radiotherapy and chemotherapy. However, the efficacy of this therapeutic strategy is not satisfactory. In-depth understanding of the molecular changes and immune infiltration in G34-DHGs will help to establish personalized tumor treatment strategies.

In this study, we conducted a comprehensive analysis of G34-DHGs at the clinicopathological and genetic level. Our research uncovered new molecular characteristics of this unique tumor, which provide potential opportunities to develop individualized therapy.

Methods

Patient Cohort

The institutional ethical committee of Sun Yat-sen University Cancer Center (SYSUCC) approved this study, and written informed consent was obtained from all patients. A flow diagram of patient selection is shown in Figure S1.

Ten H3F3A G34-mutated patients were selected from the clinicopathology database on the basis of *H3F3A* Sanger sequencing results, including nine patients with G34R mutation and one patient with G34V mutation. Pathological specimens of all patients were independently reviewed by two senior neuropathologists according to the criteria of the 2021 WHO Classification of Tumors of Central Nervous System [4]. All patients met the criteria for diffuse hemispheric glioma, H3 G34-mutant. Clinicopathological characteristics of patients including age, sex, chief complaint, site of lesion, treatment, IDH/TERT/MGMT promoter methylation status, and survival status were retrospectively reviewed.

Five cases had sufficient fresh tumor samples for whole-exome sequencing (WES) and RNA sequencing (RNA-seq); freshly frozen tumor tissues were subjected to WES and RNA-seq analyses, and corresponding blood samples were subjected to WES analyses. We also obtained WES and RNA-seq data of three Chinese patients from the Chinese Glioma Genome Atlas (CGGA) database and seven European patients from the HERBY Trial (study BO25041; clinicaltrials.gov NCT01390948).

For survival analysis, we examined overall survival (OS) of the total 20 patients with G34-DHG, along with 21 cases with *IDH*-mutant high-grade glioma and 34 cases with H3K27M-mutant diffuse midline glioma at our institution.

Hematoxylin and eosin staining and immunohistochemistry

Histological features including necrosis, nuclear atypia, mitotic activity and vascular characteristics were assessed. Immunohistochemical staining was performed using an immunostaining system (BenchMark ULTRA system, Ventana-Roche, Switzerland) with primary antibodies against GFAP (1:200, ZSGB-BIO, Beijing, China), OLIG2 (1:100, ZSGB-BIO), ATRX (1:200, ZSGB-BIO), IDH1 R132H (1:100, MX031, Fuzhou, China), H3K27M (1:1000, Millipore, Temecula, CA, USA), p53 (1:1000, Dako, Glostrup, Denmark) and Ki67 (1:200; Dako). Appropriate positive controls were included.

Methylation-specific PCR analysis

Methylation-specific PCR was conducted using an EZ DNA Methylation Kit (Zymo Research, Irvine, CA, USA) to determine the methylation status of the MGMT promoter, as described previously [5].

RNA extraction, library construction and sequencing

Total RNA was extracted using the Trizol reagent kit (Invitrogen, Carlsbad, CA, USA) in accordance with the manufacturer's protocol. RNA quality was assessed on an Agilent 2100 Bioanalyzer (Agilent Technologies, Palo Alto, CA, USA) and checked using RNase-free agarose gel electrophoresis. After total RNA was extracted, eukaryotic mRNA was enriched using Oligo(dT) beads, whereas prokaryotic mRNA was enriched by removing rRNA with the Ribo-ZeroTM Magnetic Kit (Epicentre, Madison, WI, USA). The enriched mRNA was fragmented into short fragments using fragmentation buffer and reverse transcribed into cDNA with random primers. Second-strand cDNA was synthesized by DNA polymerase I, RNase H, dNTP and buffer. The cDNA fragments were purified using the QiaQuick PCR extraction kit (Qiagen, Venlo, The Netherlands), end repaired, polyadenylated and ligated to Illumina sequencing adapters. The ligation products were size-selected by agarose gel electrophoresis, PCR amplified and sequenced using Illumina HiSeq2500 by Gene Denovo Biotechnology Co. (Guangzhou, China).

WES

DNA was extracted from fresh tissues and peripheral blood. WES was performed using a targeted capture approach with the Agilent SureSelect Human All Exon Kit (Santa Clara, CA, USA) followed by massively parallel sequencing of enriched fragments on the Illumina HiSeq2500 by Gene Denovo Biotechnology Co. Tumor and corresponding blood leukocyte DNA samples had an average sequencing depth of the target exonic region of >200×.

Somatic Variant Identification

All the sequence reads were mapped according to the human reference genome GRCh37 using BWA-MEM with default parameters. Following the GATK standard protocol, realignment and recalibration were performed for BAM files after removing PCR duplicates. Single-nucleotide variations (SNVs) were identified with MuTect in the GATK suite. Using white blood cell data as controls, tumor sample data were then input into GATK to call somatic mutations (SNV). Finally, maftools was employed to visualize the mutational landscape of the results.

Immune Infiltration Score Calculation

To de-convolute immune components of tumor samples, the TIMER online tool (http://cistrome.org/TIMER/) was employed to evaluate the immune cell infiltration score using default settings. The immune infiltration score was later visualized and plotted by the R studio function pheatmap.

Statistical Analysis

Statistical analysis was performed using IBM-SPSS Statistics version 18.0 (IBM, NY, USA). Kaplan–Meier survival curves were generated to estimate OS. Survival differences were analyzed by the log-rank test.

Results

1. Clinical Characteristics of G34-DHGs

The clinical characteristics of the 10 patients with G34-DHGs from SYSUCC are summarized in Table 1. The patient group included four male patients and six female patients. The patient age at initial diagnosis ranged from 13 to 25 years, and the median patient age was 20.5 years. The symptoms were the classic clinical features of brain tumors, including dizziness, headache, nausea, vomiting, weakness of right limbs and generalized tonic-clonic seizures dependent on the site of the lesion. All lesions were primarily located in cerebral hemispheres; the lesions were in the right hemisphere in five patients, the left hemisphere in four patients and bilateral hemisphere in one patient. Tumor invasion in the frontal lobe was detected in eight patients, and invasion in the parietal lobe was detected in three patients; temporal lobe involvement was observed in two patients and insular lobe involvement was observed in two patients. In addition, corona radiata, basal ganglia or corpus callosum were infiltrated by tumors in four patients.

For initial treatment, gross total resection (GTR) was performed in five patients, whereas four patients received subtotal resection and one patient only received biopsy. For postoperative adjuvant treatment, nine patients received adjuvant concurrent chemotherapy and radiation therapy (CCRT), and one patient who was included in a clinical trial received 12 courses of dianhydrodulcitol. Among the nine patients receiving CCRT, five patients further received maintenance temozolomide (TMZ) treatment and one patient received four courses of TMZ plus cisplatin followed by maintenance TMZ treatment.

Seven patients showed recurrent disease after the initial treatment, and four patients died. Four patients who initially received subtotal resection chose conservative treatment after recurrence, and two died at 6 and 16 months after the initial operation. The remaining three patients with recurrent disease received a second operation, and two of them further received adjuvant therapy after the second operation. Patient 9 received TG02, a novel pyrimidine-based multi-kinase inhibitor of CDKs together with JAK2 and FLT3, after STR for recurrent disease. This patient died at 1 year after recurrence with an OS of 17 months. Patient 1, who was diagnosed with methylated MGMT promoter after initially receiving GTR followed by CCRT and 12 courses of maintenance TMZ treatment, then again underwent GTR followed by radiotherapy and 12 courses of maintenance TMZ treatment for her recurrent disease; this patient achieved the longest OS of 75 months. Moreover, three patients who were also diagnosed with methylated MGMT promoter after initially receiving GTR followed by CCRT and maintenance TMZ treatment were free of recurrence after at least 18 months since the initial operation. Intriguingly, two of the three patients without recurrent disease continuously received maintenance TMZ treatment (ongoing), including patient 4, who initially received only biopsy. These results indicated that only GTR and long-term maintenance TMZ treatment might benefit patients with G34-DHG in conventional treatment.

2. Pathological Characteristics of G34-DHGs

Histopathologic examination of the surgical specimens from our cohort showed high-grade glioma morphology (Figure 1). All cases showed high cell density, featuring nuclear atypia, mitotic activity and cellular pleomorphism with focal gemistocytic cells and multinuclear giant cells. Most cases were glioblastoma (GBM)-like with microvascular proliferating and/or palisade necrosis and two cases showed focal embryonal appearance. However, calcification, perivascular growth pattern and perineuronal satellitosis, which rarely appears in GBM, were also observed (Figure 1E, F). All cases showed GFAP expression and negative expression of OLIG2; most cases were negative for ATRX (9/10) and most showed diffuse strong p53 positivity (8/10). The Ki67 labeling index was high, ranging from 20% to 60%. Sanger sequencing revealed that all cases were *IDH* wild-type and *TERT* promoter wild-type (Table 1). Methylation PCR revealed that most cases showed MGMT promoter methylation (8/10) (Table 1).

3. Mutational Landscape of G34-DHGs

To investigate the mutational landscape of G34-DHGs, we performed WES on five fresh samples and matched peripheral blood leucocytes from our cohort. The average depths of targeted exome regions in tumors and matched blood samples were 400× and 100×, respectively. More than 98.69% of the targeted regions were covered sufficiently for confident variant calling (≥10× depth). We included three G34-DHG cases from the CGGA and seven G34-DHG cases from the HERBY trial (study BO25041; clinicaltrials.gov NCT01390948). The total somatic mutations of the 15 G34-DHG samples are listed in Figure 2.

The mutational frequencies, mutation types and clinical features of the 15 G34-DHGs are displayed in Figure 2A. *TP53* (13/15 87.0%), *PDGFRA* (12/15, 80.0%) and *ATRX* (10/15, 67.0%) were the most three frequently mutated genes. Other frequently mutated genes including *MUC17* (8/15, 53.0%), *MUC16* (8/15, 53.0%), *MUC5B* (7/15, 47.0%), *MUC3A* (7/15, 47.0%), *OBSCN* (6/15, 40.0%), *SSPO* (6/15, 40.0%) and *DOCK3* (6/15, 40.0%) were identified by WES.

Notably, MUC family gene mutations have not been reported in G34-DHGs. The human MUC16 gene is located on chromosome 19p13.2 and the MUC17 gene is located on chromosome 7q22.1. Out of the eight cases with *MUC16* mutations, 87.5% (7/8) of the cases had missense mutations, and the remaining case had a frame_shift_ins mutation. Moreover, all eight cases with *MUC17* mutations had missense mutations.

Somatic SNVs and Indels

A total of 8285 exonic mutations were identified in the 15 G34-DHG patients. Of these mutations, 7187 were missense mutations, 448 were nonsense mutations, 153 were frameshift deletions, 313 were frameshift insertions, 10 were in_frame_del mutations, 1 was an in_frame_ins mutation and 173 were splice site mutations. We removed 1561 silent variants with unknown function. The predominant types of nucleotide substitutions in SNVs in G34-DHGs were C > T/G > A transitions and C > A/G > T transversions.

Oncogenic Pathways Analysis

We identified multiple pathways of somatic mutated genes in G34-DHGs using the oncogenic pathways module of the R package maftools. Crucial signal transduction pathways included the RTK-RAS, NOTCH, WNT, Hippo, PI3K, TP53, MYC and Cell_Cycle pathways (Figure 2B). Exome sequencing revealed that 14 of 15 cases had changes in the receptor tyrosine kinase RTK-RAS pathway, involving 42/84 pathway genes (including *PDGFRA*, *MET*, *BRAF*, *ERF*, *FGFR1* and *NF1*). KEGG pathway analysis revealed that many of the mutated genes were involved in cancer signal transduction. Mutant genes may promote tumor cell proliferation and escape apoptosis through cascade reaction.

Copy Number Alterations (CNAs)

We conducted somatic CNA analyses in the five SYSUCC cases and seven HEBRY cases. The results identified recurrent gains in chromosomes 3p26.33 (11/12), 4p12 (11/12), 9q21.13 (7/12) and 9q34.11 (4/12). Recurrent losses were identified in chromosomal regions 4p35.1 (10/12), 10q25.1 (10/12), 19p13.43 (9/12), 18q23 (8/12) and 9p21.3 (7/12). Loss of somatic CNAs on chromosome 10q25 affects the largest number of genes (1330 genes), including the *MGMT* locus. Gains of somatic CNAs on chromosome 3p26 affects 396 genes, including *ABCC5*. Studies have shown that ABCC5 is associated with chemoresistance of astrocytic tumors [6].

4. PDGFRA Mutation and G34-DHGs

PDGFRA is an important receptor tyrosine kinase in glial development and a recurrent driver in high-grade gliomas [7-9] *PDGFRA* mutation and the PDGFRA signaling pathway were reported to play potent oncogenic roles in G34-DHGs [10]. Our sequencing results also showed that most G34-DHGs had *PDGFRA* mutation (12/15).

To explore the potential pathways and genes related to *PDGFRA* mutation in G34-DHGs, we analyzed differentially expressed genes (DEGs) using RNA-Seq data from two G34-DHG patients with wild-type *PDGFRA* and eight G34-DHG patients with mutated *PDGFRA*. The results identified 150 DEGs (|FC| ≥2.0 and P<0.05), including 95 down-regulated genes and 55 up-regulated genes. The DEGs between the two groups are shown in a heatmap in Figure 3A. We identified the top 10 hub genes ranked by degree, including *FOS*, *CXCL8*, *CXCR1*, *IL1B*, *COL1A1*, *MMP9*, *FCGR3B*, *TNF*, *CCL4* and *CCL3*. We used MCODE in Cytoscape to identify gene modules in the PPI network and mapped the interaction network of 52 core genes in module 1 (Figure 3B). The results indicated that the genes were mainly involved with blood microparticles, the phospholipase C-activating G protein-coupled receptor signaling pathway, substrate-specific channel activity, complement and coagulation cascades, the neuroactive ligand-receptor interaction and aldosterone-regulated sodium reabsorption.

We used the DAVID database to analyze the GO and KEGG pathways of the DEGs. KEGG pathway analysis revealed that DEGs were significantly enriched in the extracellular matrix–receptor interaction, cytokine-cytokine receptor interaction, PIK3-AKT signaling pathway and chemokine signaling pathway (Figure 3C). The enriched GO-Biological Process terms included immune and inflammatory response (Figure 3D).

5. *MUC16* Mutation and Immune Infiltration Characteristics of G34-DHGs

Previous studies indicated that pHGGs with a high mutation load have an elevated neoantigen load and immune response [11,12]. However, tumors with histone H3 gene mutations are considered as immune cold tumors, which are defined as a lack of CD8 immunoreactivity and lack of tumor-infiltrating lymphocytes [13]. Using the RNA sequencing results, we next analyzed the expressions of immune-related genes in 10 patients with G34-DHGs, including 5 from SYSUCC, 3 from CGGA and 2 of the HERBY cases. The 67 differentially expressed immune-related genes were classified according to CD8+ T cell, T cell (general), B cells, monocyte, tumor-associated macrophage, M1 macrophage, M2 macrophage, neutrophil, natural killer cell, dendritic cell, Th1, Th2, Tfh, Th17, Treg and T cell exhaustion markers (Figure 4). In general, consistent with HERBY Phase II Randomized Trial, we also found G34-DHGs were immune cold tumors, with a few exceptions. For instance, the tumor specimen of patient 1 in our cohort showed significant immune infiltration with substantial amounts of CD4 and CD8 T cells (Figure S2). The OS of this patient reached 75 months, which was markedly longer than that of the nine patients with low immune infiltration (mean survival time: 12 months).

A previously published pan-cancer analysis of 30 solid tumor types showed that patients with *MUC16* mutations showed higher tumor mutation burden and neoantigen burden, indicating increased tumor immunogenicity, which can predict immune checkpoint inhibitor treatment response. The study included 397 cases of glioblastoma and 61 of these cases (15.37%) showed *MUC16* mutations [14]. Therefore, we wondered whether the *MUC16* mutation in G34-DHGs might also be associated with immune infiltration.

We used TIMER 2.0 to analyze the immune cell infiltration of G34-DHGs with *MUC16* mutation and G34-DHGs with wild-type *MUC16*. However, no connection between *MUC16* mutation and immune cell infiltration was found; this may be because of the small number of cases and relatively low immune infiltration of G34 glioma. We further analyzed the DEGs between G34-DHGs with *MUC16* mutation and G34-DHGs with wild-type *MUC16*. G Protein-Coupled Receptors (GPCR) signaling relevant proteins MTNR1B, OXTR and PDYN were all low expressed in G34-DHGs with *MUC16* mutation (Figure 5).

6. Survival Analysis of Patients with G34-DHGs

We performed survival analyses of the patients from our center (SYSUCC). We found that the OS of patients with H3G34-mutant DHGs was worse than that of patients with IDH-mutant high-grade gliomas, but better than that of patients with H3K27M-mutant DMGs. The mean survival times of patients with IDH-mutant high-grade gliomas, G34-DHGs and H3K27M DMGs were 58.4, 53.8 and 18.4 months, respectively (P<0.001).

We further performed analysis in the overall patient group (patients with G34-DHGs from SYSUCC, CGGA and HERBY Trial). Age (≥18 years old vs. <18 years old) and sex (male vs. female) did not influence patient prognosis. Although no statistical difference was achieved, Kaplan–Meier curve analyses showed some trends according to race, *PDGFRA* mutation, *MUC16* mutation and *MUC17* mutation. The median OS for Chinese patients was 18 months compared with 12 months for Caucasian patients (P = 0.105). Patients with *PDGFRA* mutation tended to show a shorter OS (median OS: 11.5 months vs. 16 months), and *MUC16* and *MUC17* mutations both seemed favorable for prognosis (median OS: 15 months vs. 12 months and 16 months vs. 11.5 months, respectively). Importantly, although immune infiltration varied in G34 glioma patients, patient 1 in our cohort who harbored MUC16 mutation had obviously high immune infiltration and achieved the longest OS of 75 months.

Discussion

Diffuse hemispheric glioma H3 G34-mutant is a newly recognized tumor type in the 2021 WHO Classification of Tumors of the Central Nervous System. This tumor is a malignant infiltrative glioma that typically occurs in the cerebral hemispheres and harbors a missense mutation in the *H3F3A* gene that results in a G34R/V substitution in histone H3. The histological heterogeneity of G34-DHGs has been previously reported [15]. In general, most cases show high-grade anaplastic features, with microscopic features of anaplastic astrocytoma, GBM or embryonic tumors (primitive neuroectodermal tumor-like features) or even anaplastic pleomorphic xanthoastrocytoma [16]. Therefore, misdiagnosis of cases is likely if clinicians and pathologists rely solely on histological diagnosis. Consistent with these findings, most cases in our center also presented as GBM-like and with/without a focal embryonal appearance. However, calcification, perivascular growth pattern and perineuronal satellitosis, which rarely appear in GBM or called 'secondary structures,' were observed [3,17]. We further analyzed the immunohistochemical and characteristics of H3G34-mutant diffuse gliomas. Lack of OLIG2 expression is one of the characteristics of this tumor and was previously reported in 100% of G34 DHGs [18]. We also observed loss of OLIG2 expression in all of our cases. In addition, loss of ATRX

expression and p53 overexpression are also frequently observed in this tumor type. The *H3F3A* G34R/V mutation is associated with a high frequency of MGMT methylation, but this is mutually exclusive with IDH or TERT promoter mutation.

We also found frequent *PDGFRA* mutation (12/15) in the G34-DHGs in our study. PDGFRA is a class III receptor tyrosine kinase with five extracellular immunoglobulin-like structures and this protein plays an important role in cell determination, cell proliferation and migration during neural development and adult neurogenesis [19,20]. Abnormal PDGFRAsignal transduction in gliomas leads to activation of the Ras-Raf-MEK-ERK pathway [21]. A high proportion of gliomas, especially TERTp wild-type GBM, are associated with somatic alterations in *PDGFRA*. Recurrent *PDGFRA* mutations have also been found in low-grade neurotumors associated with refractory seizures, called septal dysplasia neuroepithelial tumors or mucinous glial neuronal tumors [22]. These *PDGFRA* mutations include missense mutations, in-frame insertions or deletions and gene amplification. The most common variation is *PDGFRA* gene amplification, which is present in approximately one-third of HGGs. Most tumors with *PDGFRA* gene amplification have genomic deletions of exons 8 and 9 [23]. Ozawa et al reported an adult case with a gene fusion between *PDGFRA* and *VEGFR2* [24]. Point mutations are located in the extracellular domain, transmembrane domain and kinase domain of the PDGFRA receptor. These oncogenic mutations lead to constitutively activated PDGFRα, thereby activating downstream signal transduction [23-25]. In another glioma subset with histone H3 mutation (H3K27M DMGs), *PDGFRA* amplification and mutation were reported together with histone H3.3 mutation [10]. Li et al found that 18 cases of 112 midline glioma patients had *PDGFRA* mutations [26]. Both our study and the study by Chen et al found high frequencies of *PDGFRA* mutations in G34-DHGs. *PDGFRA* mutation was present in 12 out of 15 cases (80%) of our study group. Chen et al extensively analyzed 95 cases of HGGs with H3.3G34R/V mutation and found that *PDGFRA* mutations presented in 44% of all tumors and 81% of recurrent tumors. The authors speculated that *PDGFRA* mutant G34 tumors have expanded astrocytic compartments that are conducive to maintaining the active chromatin conformation state of the GSX2 enhancer to maintain high PDGFRA expression and continue to promote the carcinogenic state [10]. In GBM and in *IDH* mutant lower-grade (WHO Grades II/III) glioma, *PDGFRA* amplification is associated with shorter progression-free survival and OS and it is an independent prognostic factor [27]. *PDGFRA* amplification was also an indicator of poor prognosis in H3K27M DMGs [28,29]. However, the prognostic implication of *PDGFRA* mutation has not been extensively studied. Our data suggested that PDGFRA mutation may be an indicator for poor prognosis in G34-DHGs, but the results were not statistically significant; this may because of the relatively small number of G34 cases in our cohort.

Importantly, we found that MUC family genes were also frequently mutated in G34-DHGs. The MUC gene family encodes mucins, a type of high molecular weight glycoprotein [30]. There are 21 MUC genes in the human genome that encode secreted and membrane-type mucins [31]. Increasing evidence has shown that MUC proteins play an important role in regulating tumor cell proliferation, growth, apoptosis and chemical tolerance [32,33]. MUC gene mutation analysis showed that *MUC16* (OMIM 606154) has the highest mutation frequency in G34-DHGs, followed by *MUC17*. A pan-cancer analysis involving somatic mutations of 10195 samples and mRNA expression profiles of 9850 samples for 30 solid tumors found a greater abundance of immune cells in the microenvironment of *MUC16*-mutated tumors, and *MUC16* mutation was associated with factors associated with response to immune checkpoint inhibitor therapy [34]. Tumors with *MUC16* mutations exhibited a higher tumor mutational burden and more abundant neoantigen compared with that of *MUC16* wild-type tumors, indicating increased tumor immunogenicity. *MUC16*-mutated tumors were characterized by upregulated expression of T-effector and interferon-γ gene signature, a hallmark of preexisting immunity associated with pronounced benefit from checkpoint blockade. An additional hallmark of *MUC16*-mutated tumors is the augmented expression of multiple inhibitory checkpoints including LAG3 and others, suggesting potential adaptive immune resistance to anti-PD-1/PD-L1 therapies and that additional inhibitory pathways beyond the PD-1/PD-L1 axis might be targets. Although we discovered a high frequency of *MUC16* mutation in G34-DHGs, only one case in the *MUC16* mutation group showed abnormal high immune infiltration with abundant tumor-infiltrating lymphocytes and this patient survived up to 75 months. We did not find a relationship between *MUC16* and immune infiltration in G34-DHGs, which may be from the small sample numbers and immune-cold characteristics of G34-DHGs.

Regarding survival analysis, one study reported that the survival of patients with G34-DHGs was as poor as survival of patients with K27M DMGs [13]. However, all the cases were children in the study and the sample size was small, which may have resulted in bias. Our conclusion is consistent with most studies, showing that the OS of patients with H3 G34-mutant DHGs was worse than the survival of patients with IDH-mutant GBMs, but better than the survival of patients with H3 K27M-mutant DMGs; this may be partly because of the high frequency of MGMT promoter methylation in these tumors and favorable response to TMZ chemotherapy [8].

It is clear that histone mutations represent clearly defined entities within an umbrella HGG classification, and will require therapeutic development and clinical trials distinct. Compared with H3K27M DMGs, G34-DHGs were not sensitive to ONC-201, an effective therapeutic drug for H3K27M-DMGs [35]. Most G34-DHG patients had *MGMT* promoter methylation, and the rate was higher than the low incidence rate in H3K27M-DMGs (only one case had MGMT promoter methylation in our cohort, 1/34; data not shown), indicating that GTR and long-term maintenance TMZ treatment might benefit patients with G34-DHGs. Most cases also had *PDGFRA* mutations, and therefore the PDGFRA signaling pathway could be a potential therapeutic target. In addition, immunotherapy may be an option for cases with substantial immune infiltration and *MUC16* mutation. These important findings will lay the foundation for the future personalized treatment of G34-DHGs, thereby helping to improve the current scenario in which existing treatment methods have not significantly improved the median survival of these patients.

Conclusions

G34-DHG is a new high-grade glioma with high frequency of *PDGFRA* and *MUC* gene family mutations. PDGFRA may serve as a poor prognostic indicator and an effective therapeutic target for G34-DHGs. Moreover, *MUC16* mutation tends to be a favorable prognostic factor and indicates high immune infiltration in certain patients, which may provide a new direction for immunotherapy of G34-DHGs.

List Of Abbreviations

Diffuse hemispheric glioma H3 G34-mutant (G34-DHG), Chinese Glioma Genome Atlas database (CGGA), Hematoxylin-eosin (HE), Immunohistochemistry (IHC), Whole-exome sequencing (WES), Pediatric-type diffuse high-grade glioma (pHGG), Sun Yat-sen University Cancer Center (SYSUCC), Overall survival (OS), Gross total resection (GTR), Concurrent chemotherapy and radiation therapy (CCRT), Temozolomide (TMZ), Glioblastoma (GBM).

Declarations

Ethics approval and consent to participate

The present study was approved by the Ethical Committee of the Sun Yat-sen University Cancer Center (SYSUCC) and was carried out in accordance with the Declaration of Helsinki.

Consent for publication

Written informed consent was provided by all the included subjects.

Availability of data and materials

All data generated or analysed during this study are included in this published article. And the data is available from the corresponding author on reasonable request.

Competing interests

The authors declare that they have no competing interests.

Funding

This work was funded by the National Natural Science Foundation of China (81872324), and the Guangdong Basic and Applied Basic Research Foundation (2020A1515110069). The funders had no role in study design, data collection and analysis, decision to publish, or preparation of the manuscript.

Authors' contributions

WMH, JZ and YGM conceived and designed the experiments; HD and SZ analyzed the data; WMH, HD, SZ, JZ and YGM contributed to the writing of the manuscript. All authors read and approved the final manuscript.

Acknowledgements

We thank Gabrielle White Wolf, PhD, from Liwen Bianji (Edanz) (www.liwenbianji.cn/) for editing the English text of a draft of this manuscript.

References

1. Jones C, Perryman L, Hargrave D. Paediatric and adult malignant glioma: close relatives or distant cousins? Nat Rev Clin Oncol 2012;9(7):400-13.
2. Schwartzentruber J, Korshunov A, Liu XY, Jones DT, Pfaff E, Jacob K, Sturm D, Fontebasso AM, Quang DA, Tonjes M and others. Driver mutations in histone H3.3 and chromatin remodelling genes in paediatric glioblastoma. Nature 2012;482(7384):226-31.
3. Korshunov A, Capper D, Reuss D, Schrimpf D, Ryzhova M, Hovestadt V, Sturm D, Meyer J, Jones C, Zheludkova O and others. Histologically distinct neuroepithelial tumors with histone 3 G34 mutation are molecularly similar and comprise a single nosologic entity. Acta Neuropathol 2016;131(1):137-46.
4. Louis DN, Perry A, Wesseling P, Brat DJ, Cree IA, Figarella-Branger D, Hawkins C, Ng HK, Pfister SM, Reifenberger G and others. The 2021 WHO Classification of Tumors of the Central Nervous System: a summary. Neuro Oncol 2021;23(8):1231-1251.
5. Hu WM, Wang F, Xi SY, Zhang X, Lai JP, Wu HY, Liu LL, Sai K, Zeng J. Practice of the New Integrated Molecular Diagnostics in Gliomas: Experiences and New Findings in a Single Chinese Center. J Cancer 2020;11(6):1371-1382.
6. Bronger H, Konig J, Kopplow K, Steiner HH, Ahmadi R, Herold-Mende C, Keppler D, Nies AT. ABCC drug efflux pumps and organic anion uptake transporters in human gliomas and the blood-tumor barrier. Cancer Res 2005;65(24):11419-28.
7. Mackay A, Burford A, Carvalho D, Izquierdo E, Fazal-Salom J, Taylor KR, Bjerke L, Clarke M, Vinci M, Nandhabalan M and others. Integrated Molecular Meta-Analysis of 1,000 Pediatric High-Grade and Diffuse Intrinsic Pontine Glioma. Cancer Cell 2017;32(4):520-537.e5.
8. Sturm D, Witt H, Hovestadt V, Khuong-Quang DA, Jones DT, Konermann C, Pfaff E, Tonjes M, Sill M, Bender S and others. Hotspot mutations in H3F3A and IDH1 define distinct epigenetic and biological subgroups of glioblastoma. Cancer Cell 2012;22(4):425-37.
9. Verhaak RG, Hoadley KA, Purdom E, Wang V, Qi Y, Wilkerson MD, Miller CR, Ding L, Golub T, Mesirov JP and others. Integrated genomic analysis identifies clinically relevant subtypes of glioblastoma characterized by abnormalities in PDGFRA, IDH1, EGFR, and NF1. Cancer Cell 2010;17(1):98-110.
10. Chen C, Deshmukh S, Jessa S, Hadjadj D, Lisi V, Andrade AF, Faury D, Jawhar W, Dali R, Suzuki H and others. Histone H3.3G34-Mutant Interneuron Progenitors Co-opt PDGFRA for Gliomagenesis. Cell 2020;183(6):1617-1633.e22.
11. Gojo J, Pavelka Z, Zapletalova D, Schmook MT, Mayr L, Madlener S, Kyr M, Vejmelkova K, Smrcka M, Czech T and others. Personalized Treatment of H3K27M-Mutant Pediatric Diffuse Gliomas Provides Improved Therapeutic Opportunities. Front Oncol 2019;9:1436.
12. Indraccolo S, Lombardi G, Fassan M, Pasqualini L, Giunco S, Marcato R, Gasparini A, Candiotto C, Nalio S, Fiduccia P and others. Genetic, Epigenetic, and Immunologic Profiling of MMR-Deficient Relapsed Glioblastoma. Clin Cancer Res 2019;25(6):1828-1837.

13. Mackay A, Burford A, Molinari V, Jones D, Izquierdo E, Brouwer-Visser J, Giangaspero F, Haberler C, Pietsch T, Jacques TS and others. Molecular, Pathological, Radiological, and Immune Profiling of Non-brainstem Pediatric High-Grade Glioma from the HERBY Phase II Randomized Trial. Cancer Cell 2018;33(5):829-842.e5.
14. Zhang L, Han X, Shi Y. Association of MUC16 Mutation With Response to Immune Checkpoint Inhibitors in Solid Tumors. JAMA Netw Open 2020;3(8):e2013201.
15. Andreiuolo F, Lisner T, Zlocha J, Kramm C, Koch A, Bison B, Gareton A, Zanello M, Waha A, Varlet P and others. H3F3A-G34R mutant high grade neuroepithelial neoplasms with glial and dysplastic ganglion cell components. Acta Neuropathol Commun 2019;7(1):78.
16. Sasaki S, Tomomasa R, Nobusawa S, Hirato J, Uchiyama T, Boku E, Miyasaka T, Hirose T, Ohbayashi C. Anaplastic pleomorphic xanthoastrocytoma associated with an H3G34 mutation: a case report with review of literature. Brain Tumor Pathol 2019;36(4):169-173.
17. Yoshimoto K, Hatae R, Sangatsuda Y, Suzuki SO, Hata N, Akagi Y, Kuga D, Hideki M, Yamashita K, Togao O and others. Prevalence and clinicopathological features of H3.3 G34-mutant high-grade gliomas: a retrospective study of 411 consecutive glioma cases in a single institution. Brain Tumor Pathol 2017;34(3):103-112.
18. Wang L, Shao L, Li H, Yao K, Duan Z, Zhi C, Song S, Cheng Y, Wang F, Wang W and others. Histone H3.3 G34-mutant Diffuse Gliomas in Adults. Am J Surg Pathol 2021.
19. Chojnacki A, Mak G, Weiss S. PDGFRalpha expression distinguishes GFAP-expressing neural stem cells from PDGF-responsive neural precursors in the adult periventricular area. J Neurosci 2011;31(26):9503-12.
20. Guerit E, Arts F, Dachy G, Boulouadnine B, Demoulin JB. PDGF receptor mutations in human diseases. Cell Mol Life Sci 2021;78(8):3867-3881.
21. Roberts PJ, Der CJ. Targeting the Raf-MEK-ERK mitogen-activated protein kinase cascade for the treatment of cancer. Oncogene 2007;26(22):3291-310.
22. Chiang J, Harreld JH, Tanaka R, Li X, Wen J, Zhang C, Boue DR, Rauch TM, Boyd JT, Chen J and others. Septal dysembryoplastic neuroepithelial tumor: a comprehensive clinical, imaging, histopathologic, and molecular analysis. Neuro Oncol 2019;21(6):800-808.
23. Paugh BS, Zhu X, Qu C, Endersby R, Diaz AK, Zhang J, Bax DA, Carvalho D, Reis RM, Onar-Thomas A and others. Novel oncogenic PDGFRA mutations in pediatric high-grade gliomas. Cancer Res 2013;73(20):6219-29.
24. Ozawa T, Brennan CW, Wang L, Squatrito M, Sasayama T, Nakada M, Huse JT, Pedraza A, Utsuki S, Yasui Y and others. PDGFRA gene rearrangements are frequent genetic events in PDGFRA-amplified glioblastomas. Genes Dev 2010;24(19):2205-18.
25. Velghe AI, Van Cauwenberghe S, Polyansky AA, Chand D, Montano-Almendras CP, Charni S, Hallberg B, Essaghir A, Demoulin JB. PDGFRA alterations in cancer: characterization of a gain-of-function V536E transmembrane mutant as well as loss-of-function and passenger mutations. Oncogene 2014;33(20):2568-76.
26. Li H, Shan C, Wu S, Cheng B, Fan C, Cai L, Chen Y, Shi Y, Liu K, Shao Y and others. Genomic Profiling Identified Novel Prognostic Biomarkers in Chinese Midline Glioma Patients. Front Oncol 2020;10:607429.
27. Pathania M, De Jay N, Maestro N, Harutyunyan AS, Nitarska J, Pahlavan P, Henderson S, Mikael LG, Richard-Londt A, Zhang Y and others. H3.3(K27M) Cooperates with Trp53 Loss and PDGFRA Gain in Mouse Embryonic Neural Progenitor Cells to Induce Invasive High-Grade Gliomas. Cancer Cell 2017;32(5):684-700.e9.
28. Yang RR, Shi ZF, Zhang ZY, Chan AK, Aibaidula A, Wang WW, Kwan J, Poon WS, Chen H, Li WC and others. IDH mutant lower grade (WHO Grades II/III) astrocytomas can be stratified for risk by CDKN2A, CDK4 and PDGFRA copy number alterations. Brain Pathol 2020;30(3):541-553.
29. Dufour C, Perbet R, Leblond P, Vasseur R, Stechly L, Pierache A, Reyns N, Touzet G, Le Rhun E, Vinchon M and others. Identification of prognostic markers in diffuse midline gliomas H3K27M-mutant. Brain Pathol 2020;30(1):179-190.
30. Imai Y, Yamagishi H, Fukuda K, Ono Y, Inoue T, Ueda Y. Differential mucin phenotypes and their significance in a variation of colorectal carcinoma. World J Gastroenterol 2013;19(25):3957-68.
31. Boltin D, Perets TT, Vilkin A, Niv Y. Mucin function in inflammatory bowel disease: an update. J Clin Gastroenterol 2013;47(2):106-11.
32. Jiang Z, Wang H, Li L, Hou Z, Liu W, Zhou T, Li Y, Chen S. Analysis of TGCA data reveals genetic and epigenetic changes and biological function of MUC family genes in colorectal cancer. Future Oncol 2019;15(35):4031-4043.
33. Ringel J, Lohr M. The MUC gene family: their role in diagnosis and early detection of pancreatic cancer. Mol Cancer 2003;2:9.
34. Zhang L, Han X, Shi Y. Association of MUC16 Mutation With Response to Immune Checkpoint Inhibitors in Solid Tumors. JAMA Netw Open 2020;3(8):e2013201.
35. Wierzbicki K, Ravi K, Franson A, Bruzek A, Cantor E, Harris M, Homan MJ, Marini BL, Kawakibi AR, Ravindran R and others. Targeting and Therapeutic Monitoring of H3K27M-Mutant Glioma. Curr Oncol Rep 2020;22(2):19.

Table

Table 1. Clinical characteristics of 10 SYSUCC patients with H3 G34-mutant diffuse hemispheric gliomas

	Patient 1	Patient 2	Patient 3	Patient 4	Patient 5	Patient 6	Patient 7	Patient 8
Sex/age (years)	F/14	F/18	M/16	F/20	M/25	F/23	F/23	M/13
Chef complaint	Headache, nausea and vomiting	Headache, nausea and vomiting	Weakness of right limbs	Generalized tonic clonic seizures	Generalized tonic clonic seizures	Headache, nausea and vomiting	Headache and weakness of left limbs	Dizziness and weakness of right foot
Site of lesion	Left temporal lobe	Right frontal lobe	Left parietal lobe and corpus callosum	Bilateral frontal lobe and corpus callosum	Right frontal, temporal, insular lobe and basal ganglia	Right frontal lobe、corona radiata, basal ganglia and corpus callosum	Right frontal and insular lobe	Left frontal and parietal lobe
Initial OP and adjuvant Tx	GTR+CCRT+ TMZ#12	GTR+CCRT+ TMZ#2	STR+CCRT	Biopsy+CCRT+ TMZ#24 (continuously)	GTR+CCRT+ TMZ#22 (co(continuously)	STR+CCRT	STR+CCRT	STR+CCRT+ TMZ/DDP#4+ TMZ#6
2nd OP and adjuvant Tx	GTR+RT+TMZ#12	NA	Conservative	NA	NA	Conservative	Conservative	Conservative
H3F3A	G34R	G34R	G34V	G34R	G34R	G34R	G34R	G34R
MGMT promoter	Methylated	Methylated	Un-methylated	Methylated	Methylated	Methylated	Methylated	Methylated
IDH	Wildtype	Wildtype	Wildtype	Wildtype	Wildtype	Wildtype	Wildtype	Wildtype
TERT promoter	Wildtype	Wildtype	Wildtype	Wildtype	Wildtype	Wildtype	Wildtype	Wildtype
Morphology	GBM with primitive neuronal component	GBM	GBM	GBM	GBM	GBM	GBM	GBM
Current status	Death	Alive	Death	Alive	Alive	Death	Alive	Alive
OS (months)	75	24	16	21	18	6	16	13

CCRT concurrent chemotherapy and radiation therapy, DDP cisplatin, GBM glioblastoma, GTR gross total resection, MGMT O6 -methylguanine-DNA methyltransferase, NA not applicable, RT radiation therapy, STR subtotal resection, TMZ temozolomide.

Figures

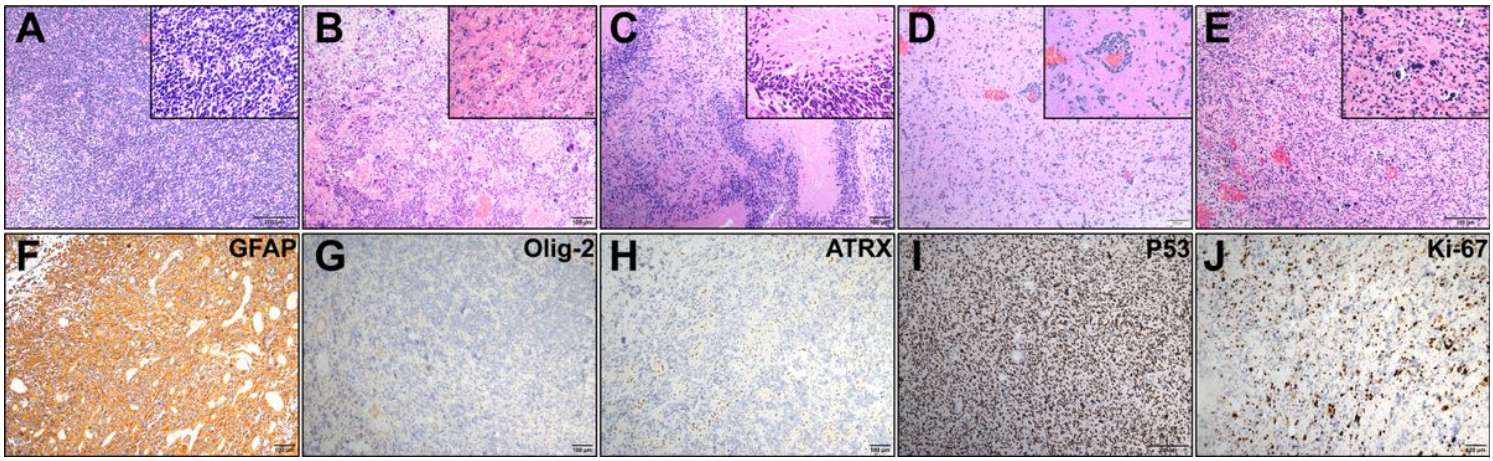

Figure 1

Histological analysis of diffuse hemispheric glioma H3 G34-mutant specimens. Hematoxylin and eosin staining shows embryonal appearance/small cell glioblastoma-like morphology (A), giant cell glioblastoma-like morphology (B), palisade necrosis (C), perivascular growth pattern (D) and calcification (E). (F–J) Immunohistochemistry for the indicated proteins.

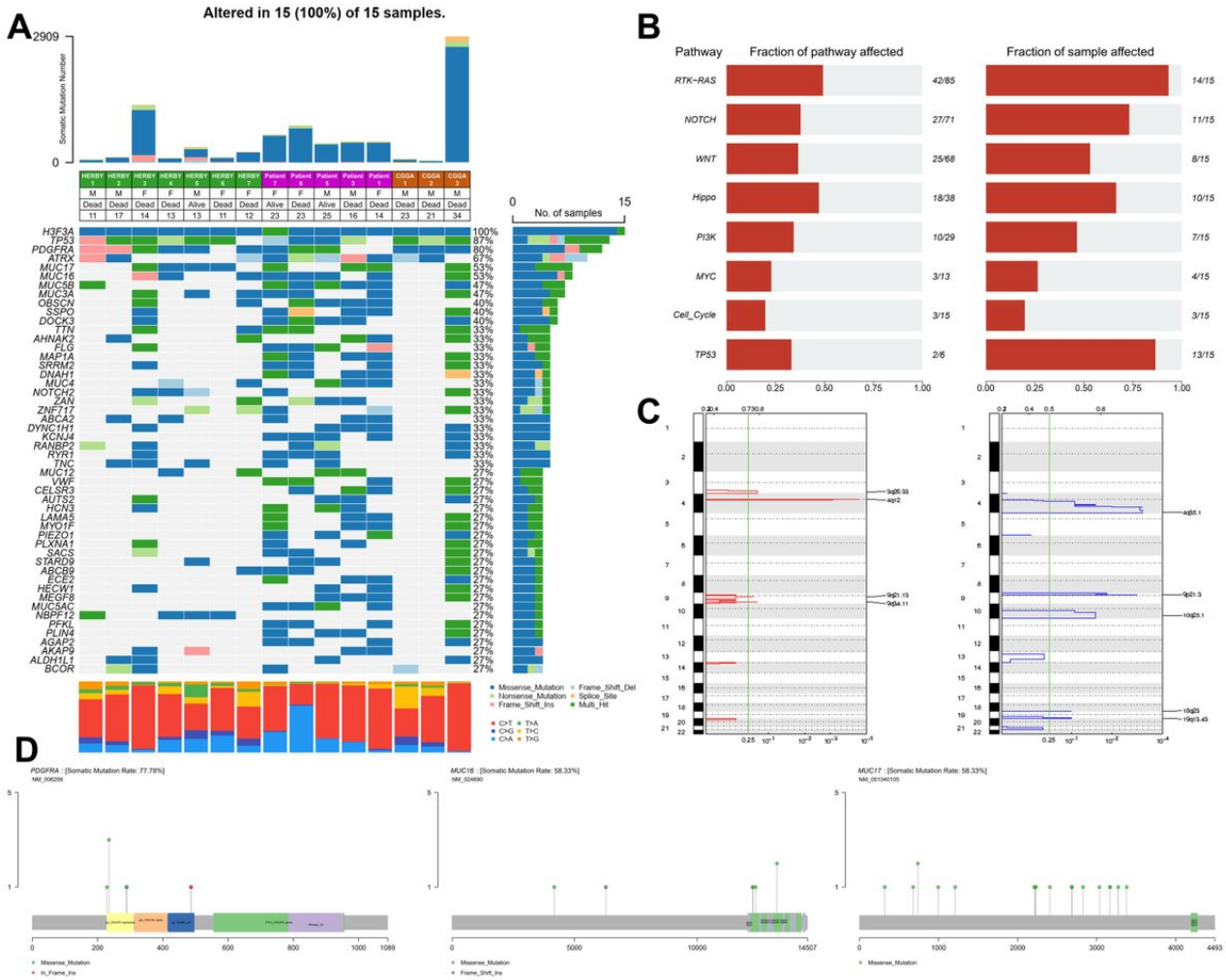

Figure 2

Mutation spectrum of diffuse hemispheric glioma H3 G34-mutant tumors. A. The total somatic mutations of 15 diffuse hemispheric glioma H3 G34-mutant specimens. Red represents C > T/G > A mutations, blue represents C > G/G > C mutations, green represents T > C/A > G mutations, purple represents C > A/G > T mutations, orange represents T > G/A > C mutations, and yellow represents T > A/ A > T mutations. The percentages indicate the proportion of samples with the mutations. B. The pathways most commonly affected by genetic mutations in diffuse hemispheric glioma H3 G34-mutant tumors included RTK-RAS, NOTCH, WNT, Hippo, PI3K, TP53, MYC and Cell_Cycle pathways. Left: histogram shows the number of mutations in each pathway. Right: histogram represent the fraction of samples affected. C. Recurrent copy number alterations. GISTIC2.0 plot of recurrent focal losses (a) and gains (b). Chromosomes are represented along the vertical axis; q values are marked along the horizontal axis. The green lines mark the cut-off for the significance threshold (q = 0.25). D. Schematics showing the locations of the missense mutations and truncating mutations on the PDGFRA (left), MUC16 (middle) and MUC17 (right) genes.

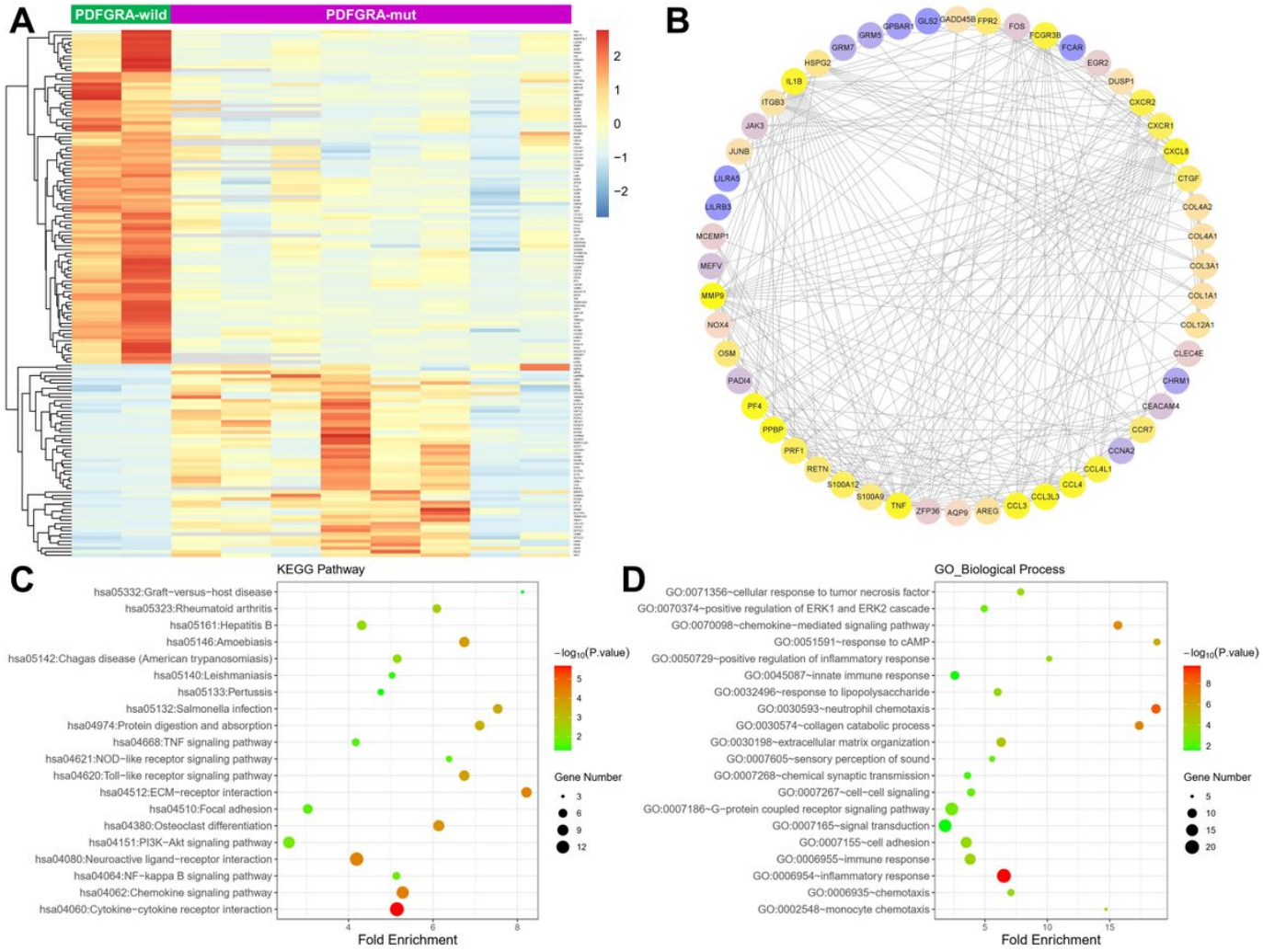

Figure 3

Analysis of differentially expressed genes in diffuse hemispheric glioma H3 G34-mutant tumors with PDGFRA mutation. Differential gene expression in two G34-DHG patients with wild-type PDGFRA and eight G34-DHG patients with mutated PDGFRA (A). Protein-protein interactions of the differentially expressed genes (B), KEGG pathway analysis (C) and GO-Biological process analysis (D).

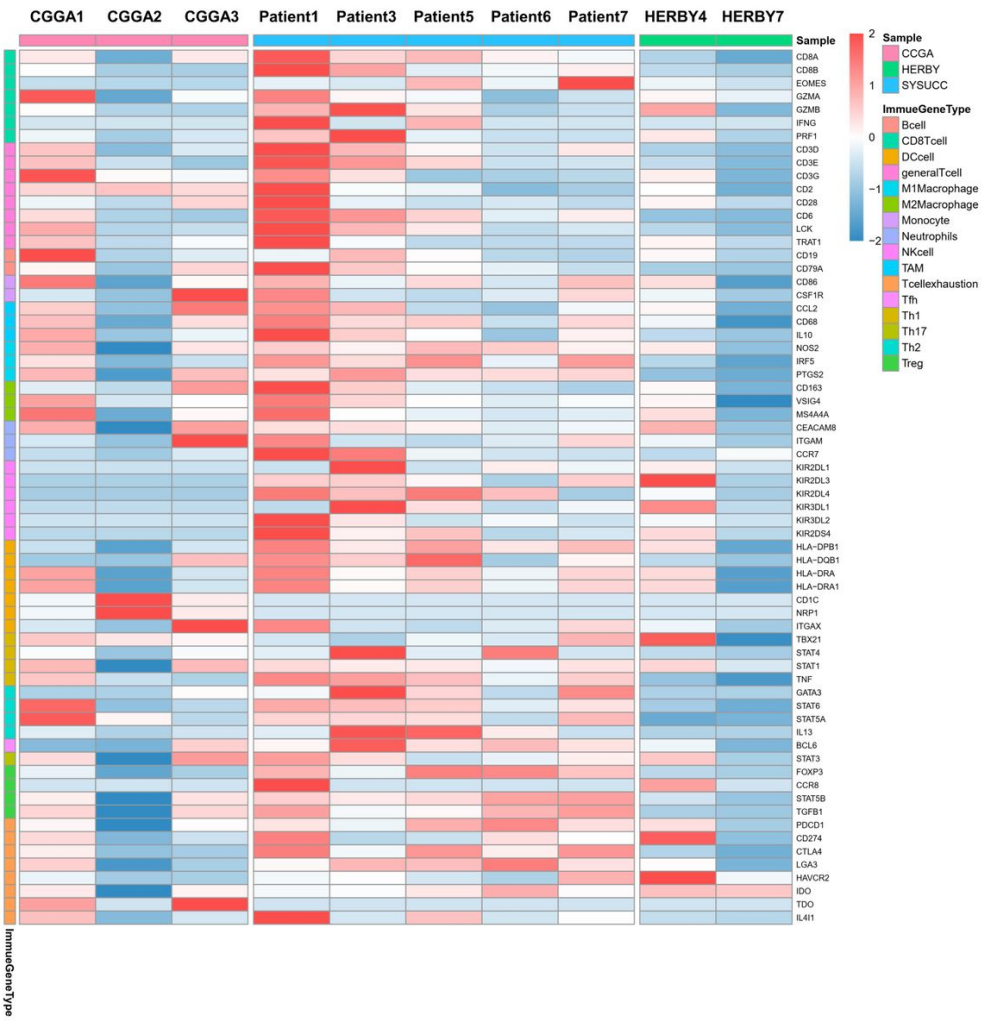

Figure 4

Immune-related genes expression profiles for immune cells plotted as a heatmap from 10 cases with RNA-seq data.

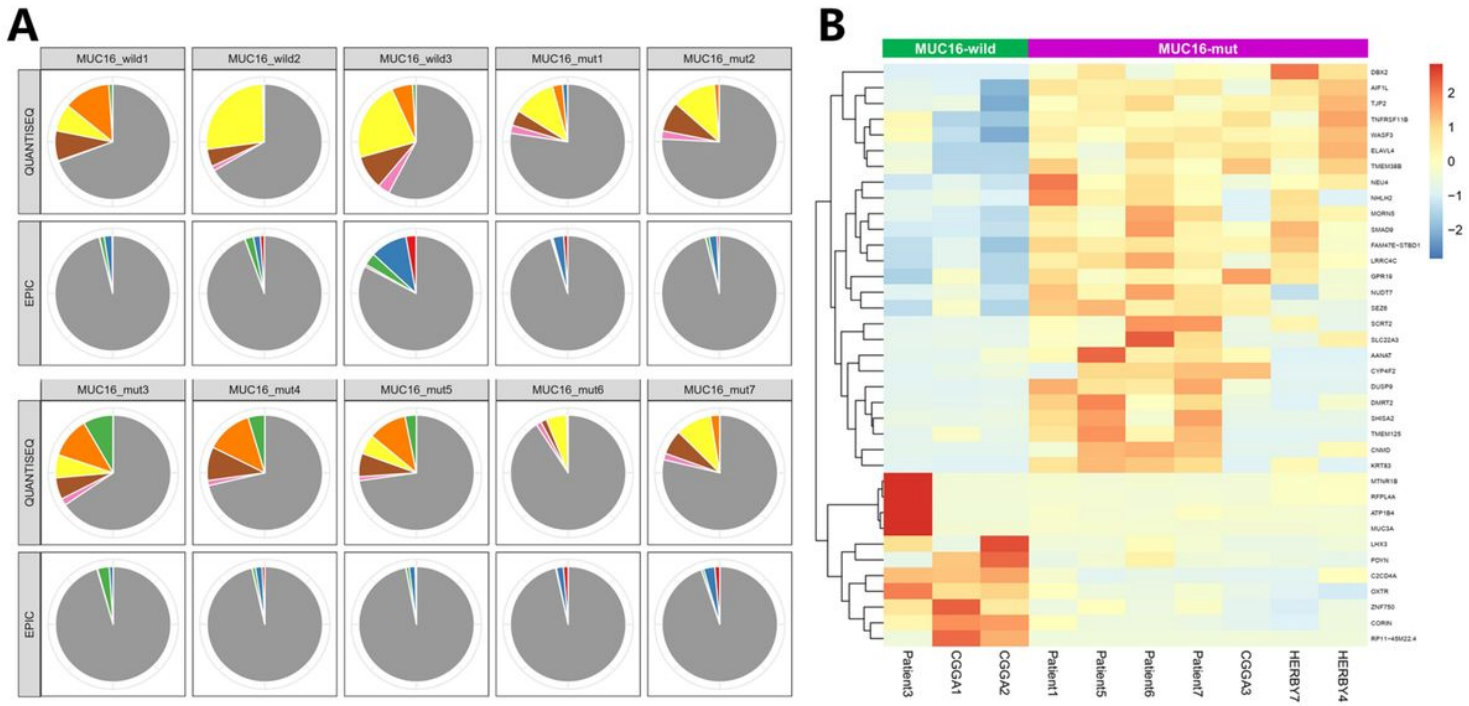

Figure 5

Immune gene expression signatures and differential genes for MUC16 mutant and wild-type diffuse hemispheric glioma H3 G34-mutant tumors. A. A multi-panel pie plot showing the proportion of immune cell types in MUC16 mutant and wild-type samples. The eight immune cell types are highlighted in different colors. B. Differential gene expression types in MUC16 mutant and wild-type cases.

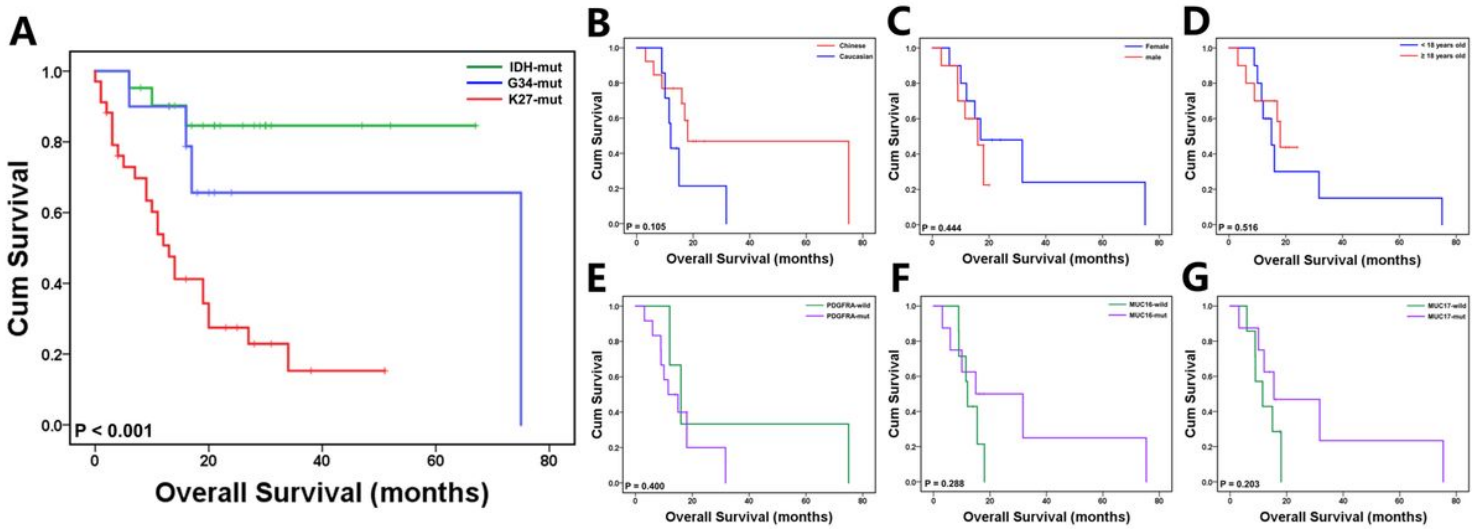

Figure 6

Kaplan–Meier curves of overall survival (OS) A. Overall survival analysis of patients with G34-DHGs compared with patients with IDH-mutant HGGs and patients with H3K27M DMGs in our cohort (SYSUCC); B. overall survival of Chinese (SYSUCC+CGGA) and Caucasian (HERBY Trail) patients with diffuse hemispheric glioma H3 G34-mutant tumors; C. overall survival of male patients and female patients in the overall patient group (SYSUCC+CGGA+HERBY Trail); D. overall survival according to age (age ≥ 18 years vs. < 18 years) in the overall patient group (SYSUCC+CGGA+HERBY Trail); E. overall survival according to PDGFRA mutation (PDGFRA mutation vs. PDGFRA wild-type) in G34 WES cases; F. overall survival according to MUC16 mutation (MUC16 mutated vs. MUC16 wild-type) in G34 WES cases; G. overall survival according to MUC17 mutation (MUC17 mutated vs. MUC17 wild-type) in G34 WES cases

Supplementary Files

This is a list of supplementary files associated with this preprint. Click to download.

- FigureS1.jpg
- FigureS2.jpg